Supplemental Material for:

**Pericentrin deficiency in smooth muscle cells augments atherosclerosis through HSF1-driven cholesterol biosynthesis**

Suravi Majumder, Abhijnan Chattopadhyay, Jamie M. Wright, Pujun Guan, L. Maximillian Buja, Callie S. Kwartler, Dianna M. Milewicz.

This file contains:

Supplemental tables 1-2

Supplemental figures 1-7

**Supplemental Table 1**

**Animals**

| Species | Vendor or Source | Background Strain | Sex | Persistent ID / URL |
|---|---|---|---|---|
| *Mus musculus* *Pcnt*$^{floxed/floxed}$ | This paper | C57BL/6J and 129S4/SvJaeSor | M/F | N/A |
| *Mus musculus* STOCK B6.Cg-Tg(Tagln-cre)1Her/J | The Jackson Laboratory | C57BL/6J | M/F | https://www.jax.org/strain/017491 |

**Supplemental Table 2**

**SYBR Green primers for qPCR**

| **Gene** | **Forward primer (5' -> 3')** | **Reverse primer (5' -> 3')** |
|---|---|---|
| *18s rRNA* | GTAACCCGTTGAACCCCATT | CCATCCAATCGGTAGTAGCG |
| *Atf4* | GGGTTCTGTCTTCCACTCCA | AAGCAGCAGAGTCAGGCTTTC |
| *Fdps* | GGAGGTCCTAGAGTACAATGCC | AAGCCTGGAGCAGTTCTACAC |
| *Fn1* | CGAGGTGACAGAGACCACAA | CTGGAGTCAAGCCAGACACA |
| *Hmgcr* | TGTCCCCACTATGACTTCCC | TCGGTGGCCTCTAGTGAGAT |
| *Hmgcs1* | TGGCAGGGAGTCTTGGTACT | TCCCACTCCAAATGATGACA |
| *Hsp90aa1* | AATGCTTAGAACTATTTACTGAACTAGCAGAA | GTCCTCGTGAATTCCAAGCTTT |
| *Hsp90ab1* | GCGCACGCTGACTTTGGT | CCTGGAGAGCCTCCATGAAC |
| *Hspa1a* | CAGCGAGGCTGACAAGAAGAA | GGAGATGACCTCCTGGCACT |
| *Idi1* | GGTTCAGCTTCTAGCGGAGA | TCGCCTGGGTTACTTAATGG |
| *Klf4* | CTGAACAGCAGGGACTGTCA | GTGTGGGTGGCTGTTCTTTT |
| *Lgals3* | AGGAGAGGGAATGATGTTGCC | GGTTTGCCACTCTCAAAGGG |
| *Ly6a* | TCAGGAGGCAGCAGTTATTGTGGA | TACATTGCAGAGGTCTTCCTGGCA |
| *Mvd* | ATGGCCTCAGAAAAGCCTCAG | TGGTCGTTTTTAGCTGGTCCT |

| | | |
|---|---|---|
| *Pcnt* | GAGGAGAAGTCGGTCTTGTGGA | GCGGTCCTTTTCAGACTGCTTC |
| *Vcam1* | CCGGCATATACGAGTGTGAA | GATGCGCAGTAGAGTGCAAG |
| *Xbp1 (spliced)* | CTGAGTCCGAATCAGGTGCAG | GTCCATGGGAAGATGTTCTGG |
| *Xbp1 (unspliced)* | CAGCACTCAGACTATGTGCA | GTCCATGGGAAGATGTTCTGG |

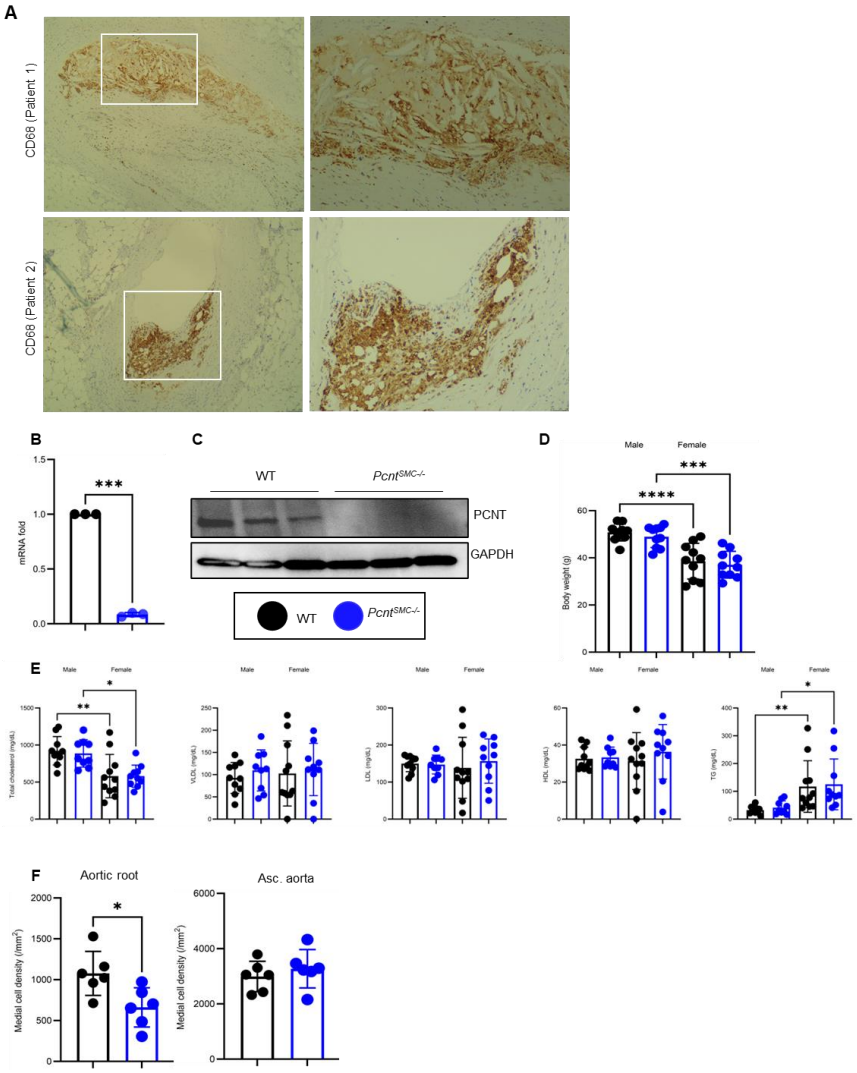


**Supplemental Figure 1. Loss of *Pcnt* from SMCs augments atherosclerosis. (A)** Coronary artery atherosclerotic lesions of two MOPDII patients show positive staining for CD68 (scale bars: left panels - 250μm, right panels – 100μm). **(B, C)** *Pcnt* mRNA expression (**B**, analyzed by unpaired student's t-test followed by Welch's correction) and immunoblotting confirm successful deletion of PCNT protein from SMCs (**C**)**. (D**) Male mice of both genotypes exhibit significantly higher body weights compared to their corresponding females after 12 week HFD (analyzed by 2-way ANOVA followed by Tukey's multiple comparisons test)**.** (**E**) FPLC analysis of serum samples demonstrated no significant difference in total cholesterol, VLDL, LDL, HDL and triglyceride (TG) levels between $Pcnt^{SMC-/-}$ and WT mice. Female mice of both genotypes have lower total cholesterol and higher TG compared to their corresponding male mice. N=10 per genotype, per sex. All data were analyzed by 2-way ANOVA followed by Tukey's multiple comparisons test, except for TG, which was analyzed using Kruskal-Wallis test followed by Dunn's multiple comparisons test. (**F**) Aortic roots of $Pcnt^{SMC-/-}$ mice showed significantly lower medial cell density compared to WT mice, but no difference was observed in the ascending aortas (unpaired student's t-test followed by Welch's correction). All gene expression data are representative of three independent experiments. Error bars represent standard deviation. *, **, ***, **** - p <0.05, 0.01, 0.001 and 0.0001 respectively.

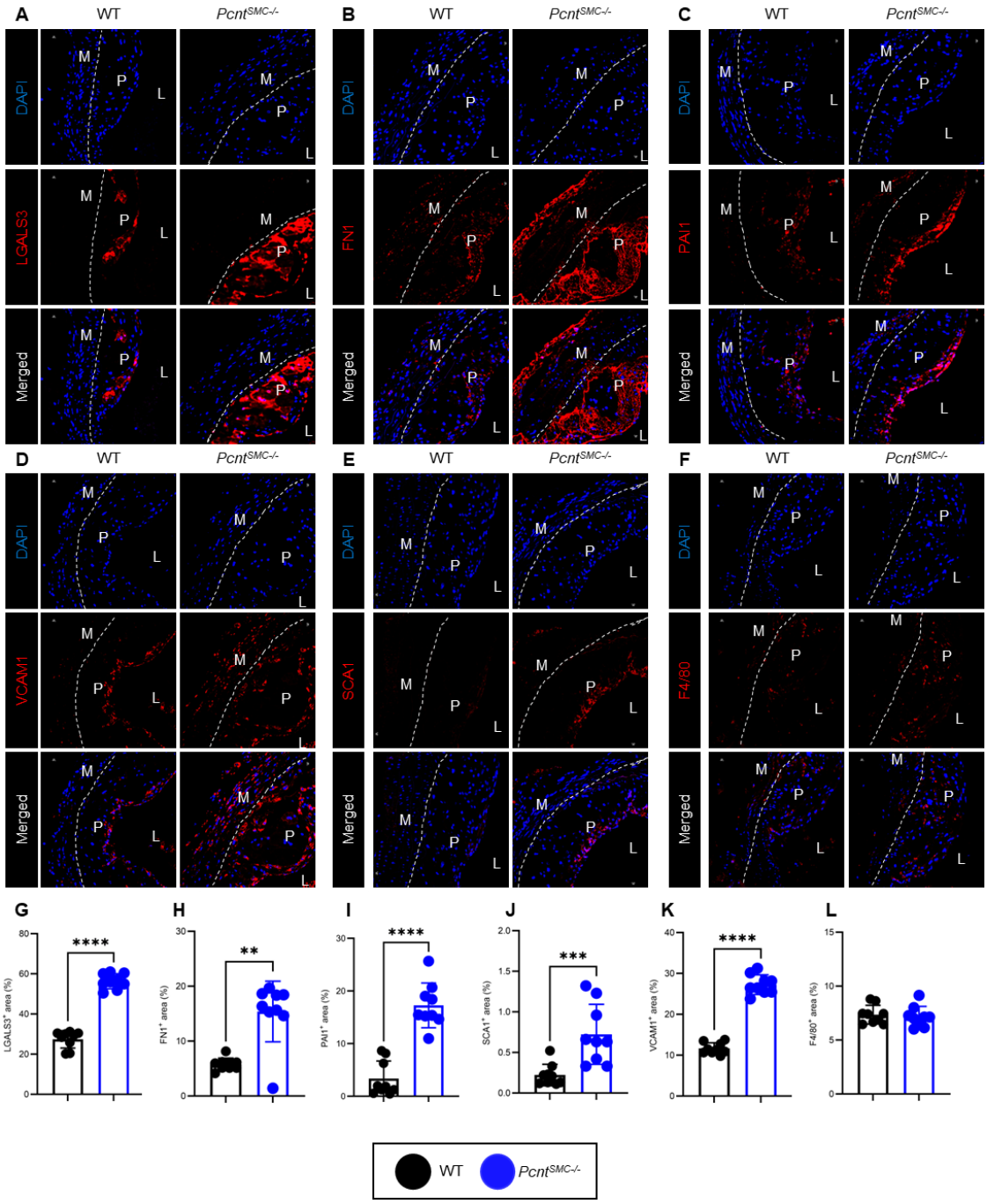


**Supplemental Figure 2. *Pcnt*$^{SMC-/-}$ mice show significantly increased expression of SMC modulation markers in ascending aorta lesions**. (**A-F**) Immunohistochemical staining of ascending aortic sections against SMC modulation markers LGALS3, FN1, PAI1, VCAM1, SCA1 and the macrophage marker F4/80 (counterstained with DAPI, blue), shows significantly higher staining for all modulation markers except SCA1, and no change in staining for F4/80 in *Pcnt*$^{SMC-/-}$ mice compared to WT mice, as quantified in **G-L.** (N=9, quantification for LGALS3, FN1, PAI1, SCA1, and F4/80 were analyzed by unpaired student's t-test followed by Welch's correction, and that for VCAM1 was analyzed by Mann Whitney U-test). Error bars represent standard deviation. **** - $p < 0.0001$. L, lumen; M, medial layer; and P, plaque. Scale bar – 5μm.

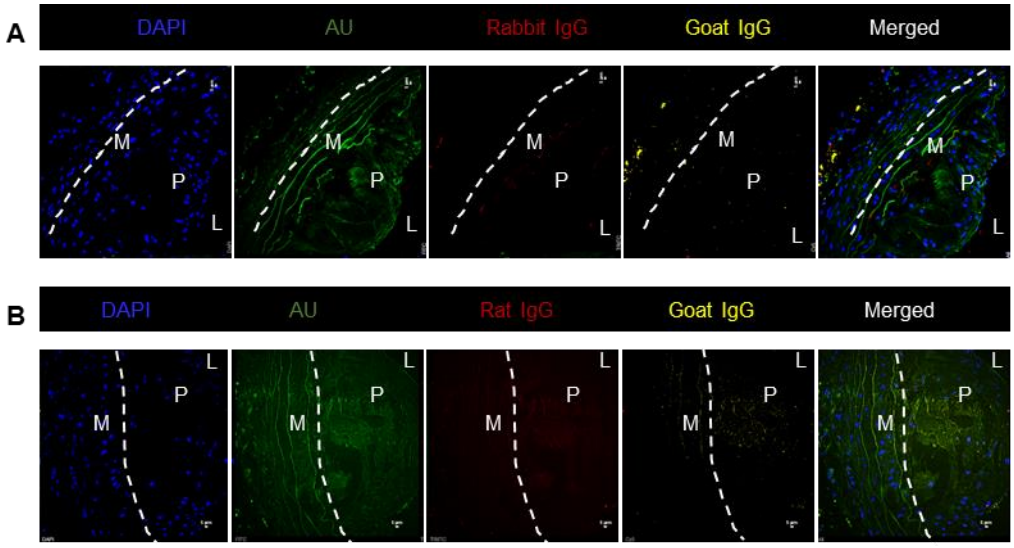


**Supplemental Figure 3. Negative controls for immunostaining experiments. (A,B)** Aortic sections were stained with normal goat, rabbit or rat IgG to ensure specificity of goat, rabbit and rat antibodies used for immunostaining. Scale bar – 5μm.

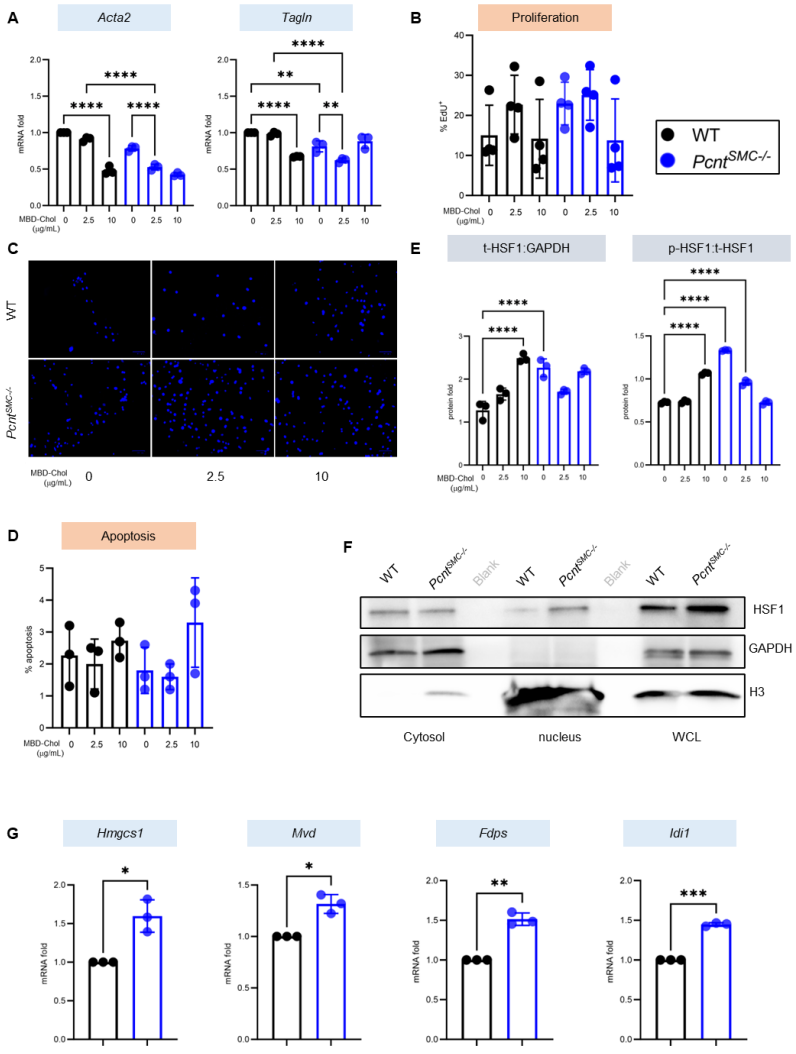


**Supplemental Figure 4. Augmented phenotypic modulation of *Pcnt*$^{SMC-/-}$ SMCs is due to increased HSF1 activation driving cholesterol biosynthesis.** (**A**) Expression of contractile makers (*Acta2*, *Tagln*) is reduced at baseline or with exposure to 2.5μg/mL MBD-Chol in *Pcnt*$^{SMC-/-}$ SMCs, compared to with 10μg/mL MBD-Chol in WT SMCs. (**B**) No difference in proliferation, measured by EdU incorporation, is observed between *Pcnt*$^{SMC-/-}$ and WT SMCs. (**C**) *Pcnt*$^{SMC-/-}$ SMCs exhibit higher migration both at baseline and with exposure to MBD-Chol, as demonstrated by DAPI staining of the nuclei of migrated cells (quantified in Main Fig. 4F). (**D**) Flow cytometry analysis of annexin V cells shows no change in apoptosis between genotypes or with cholesterol treatment. (**E**) Quantification of total and phosphorylated HSF1 (p-HSF1) protein levels. Representative blot is shown In Figure 4C. (**F**) Western blots of fractionated lysates show increased nuclear levels of HSF1 in *Pcnt*$^{SMC-/-}$ SMCs. (**G**) Expression of cholesterol biosynthesis pathway genes, *Hmgcs1*, *Mvd*, *Fdps*, *Idi1*, was significantly elevated in *Pcnt*$^{SMC-/-}$ SMCs. Data analyzed by unpaired t-test with Welch's correction. All gene expression data are representative of three independent experiments. Error bars represent standard deviation. All data in A, B and D were analyzed by 2-way ANOVA followed by Tukey's multiple comparisons test, and those in E by unpaired student's t-test followed by Welch's correction. *, **, ***, **** - p <0.05, 0.01, 0.001 and 0.0001 respectively. WCL, whole cell lysates.

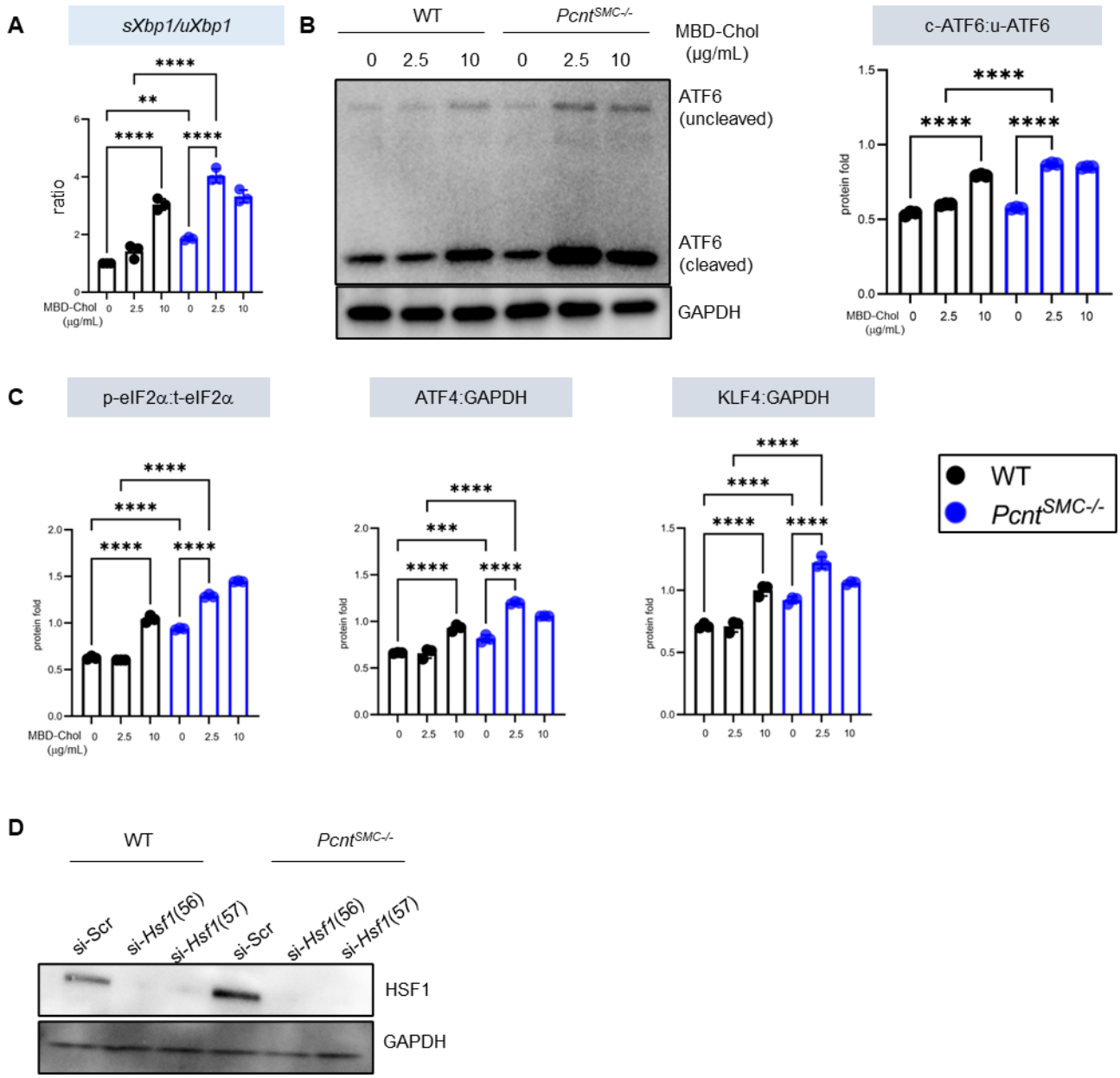


**Supplemental Figure 5.** ***Pcnt*** **deletion-induced augmented UPR, PERK signaling and SMC phenotypic modulation are HSF1-dependent**. **A,B)** Increased splicing of *Xbp1* (s*Xbp1*/u*Xbp1* ratio) (**A**) and ATF6 cleavage (**B**) demonstrate activation of IRE1α and ATF6 signaling respectively at baseline in *Pcnt*$^{SMC-/-}$ SMCs. (**C**) Quantification of total and phospho-eIF2α, ATF4 and KLF4**.** Confirmation of si-RNA mediated knock down of HSF1. Representative blot is shown in Figure 5B **D)** Western blot confirms knockdown efficiency of two siRNAs directed against *Hsf1*. All data were analyzed by 2-way ANOVA followed by Tukey's multiple comparisons test. All gene expression data are representative of three independent experiments. Error bars represent standard deviation. **, ***, **** - p <0.01, 0.001 and 0.0001 respectively.

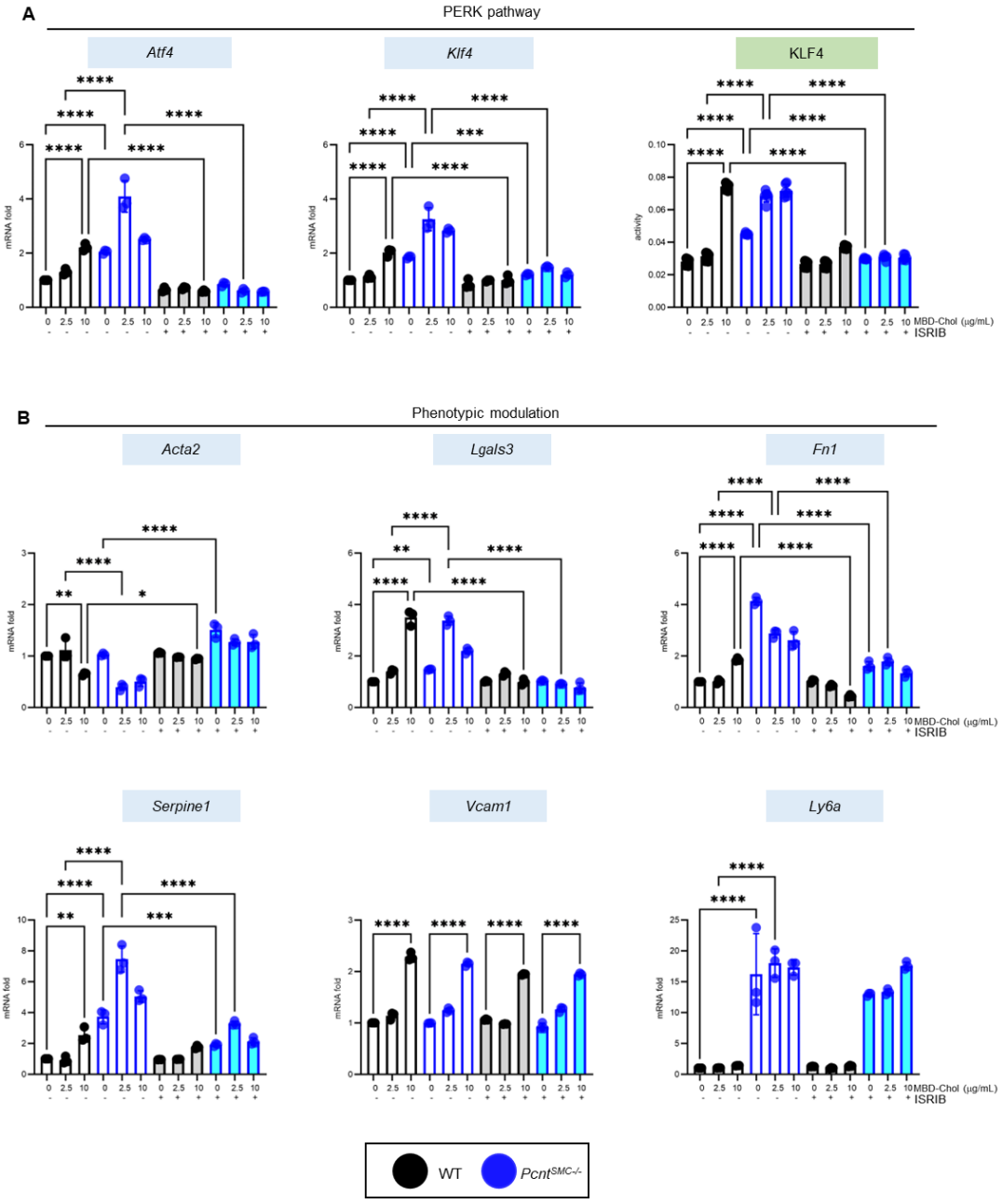


**Supplemental Figure 6. Inhibition of PERK signaling reverses augmented phenotypic modulation in *Pcnt*$^{SMC-/-}$ SMCs.** (**A**) Treatment with the PERK inhibitor, ISRIB reverses the upregulation of PERK signaling and augmented phenotypic modulation in *Pcnt*$^{SMC-/-}$ SMCs: (*Atf4, Klf4* expression and KLF4 activity). (**B**) Treatment with the PERK inhibitor, ISRIB rescues decreased expression of a contractile marker (*Acta2*) and upregulation of all modulation markers except *Vcam1* and *Ly6a*. All data analyzed by two way ANOVA followed by Tukey's multiple comparisons test. All gene expression data are representative of three independent experiments. Error bars represent standard deviation. *, **, ***, **** - p <0.05, 0.01, 0.001 and 0.0001 respectively.

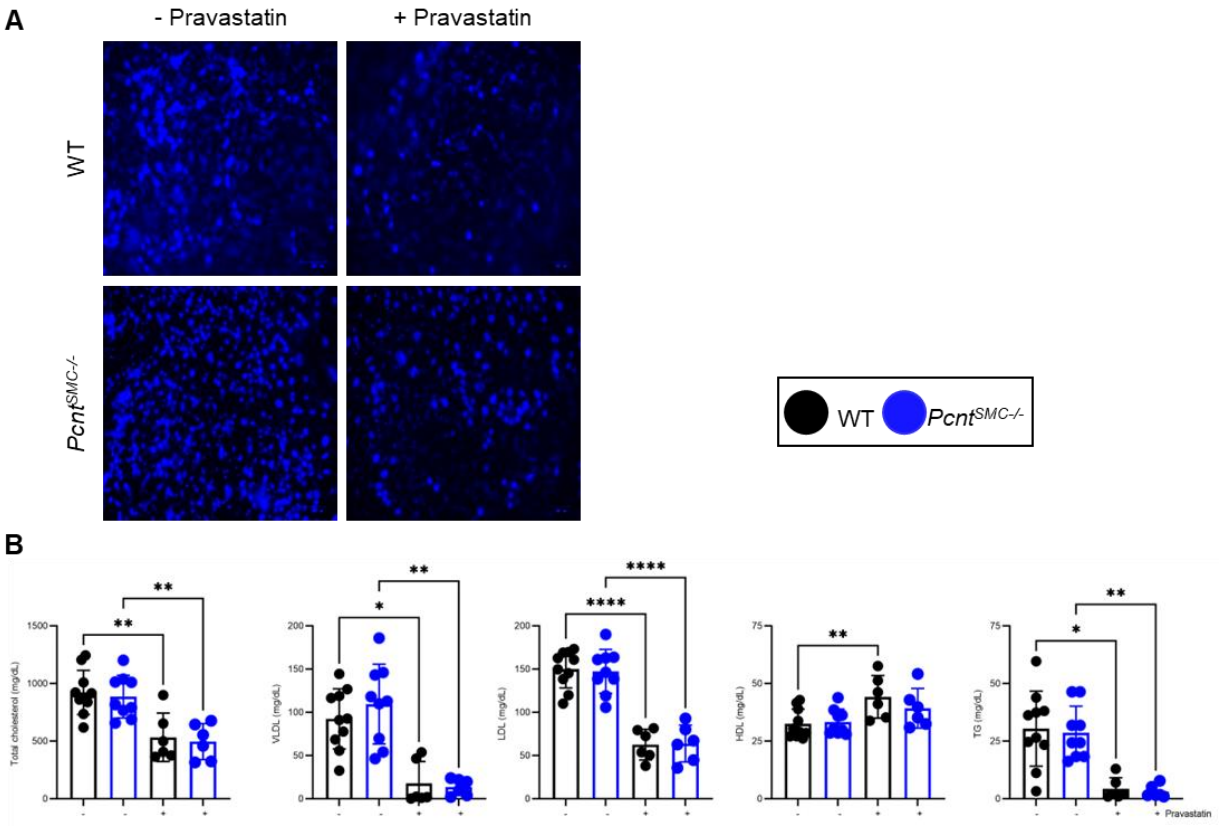


**Supplemental Figure 7. Treatment with the HMGCR inhibitor pravastatin reduces migration in *Pcnt*$^{SMC-/-}$ SMCs and serum phospholipids in *Pcnt*$^{SMC-/-}$ mice.** (**A**) Pravastatin treatment reduces migration in both *Pcnt*$^{SMC-/-}$ and WT SMCs, quantification show in Figure 6D. (**B**) Lipid profile analysis demonstrated that pravastatin treatment reduced total cholesterol, very low density lipoprotein (VLDL), low density lipoprotein (LDL) and triglyceride (TG) levels in both *Pcnt*$^{SMC-/-}$ and WT mice to a similar extent. N=10 per genotype per treatment. Data was analyzed using Kruskal-Wallis test followed by Dunn's multiple comparisons test for VLDL and TG, and using 2-way ANOVA followed by Tukey's multiple comparisons test for total cholesterol, LDL, and HDL. Error bars represent standard deviation. *, **, **** - p <0.05, 0.01, and 0.0001 respectively.